



Partial Transmit Sequence Chaotic Sand Cat Swarm Optimization Based Phase Optimizer for Peak-to-Average Power Ratio Reduction

Sowmyashree Mandya Siddegowda^{1*} Sharath Sampaih¹

¹*Department of Electronics and Communication, Government Engineering College Chamarajanagar, India*

* Corresponding author's Email: Sowmya.mtech@mail.com

Abstract: Orthogonal Frequency Division Multiplexing (OFDM) is the most significant transmission techniques that permits feasible modulation and demodulation. OFDM system is majorly affected by high Peak-to-Average Power Ratio (PAPR) values. To reduce this issue, this research proposed a Partial Transmit Sequence - Chaotic Sand Cat Swarm Optimization (PTS-CSCSO) technique of Cyclic Prefix-OFDM (CP-OFDM). To encode and decode the signal in the CP-OFDM system, the Space Time Block Coding (STBC) technique is utilized and for modulation and demodulation, the Quadrature Amplitude Modulation (QAM-16) is utilized. The PTS technique is utilized for PAPR reduction, in that phase factor is optimized by using the proposed PTS-CSCSO algorithm. The Additive White Gaussian Noise (AWGN) channel is utilized, that transmit the signal from transmitter to receiver. The performance of the proposed algorithm is evaluated with performance metrics of Bit Error Rate (BER), Symbol Error Rate (SER), and Complementary Cumulative Distribution Function (CCDF). The proposed algorithm attained a minimum BER of 10^{-8} which is superior to other existing methods like Prime Learning Ant Lion Optimization (PL-ALO) and Phase Optimizer-assisted Partial Transmit Sequence (PO-PTS).

Keywords: Additive white Gaussian noise, Chaotic sand cat swarm optimization, Orthogonal frequency division multiplexing, Partial transmit sequence and peak-to-average power ratio.

1. Introduction

In recent times, numerous improvements and extreme adjustments have been continuously utilized for wireless communication to enhance its quality and make it a much more dependable technology [1]. Orthogonal Frequency Division Multiplexing (OFDM) contains high spectral effectiveness and provides high security against immunity to multiple paths vanishing [2], hence OFDM is introduced in wireless communication [3-5]. Additionally, OFDM is taken as an efficient key to introduce a 5G mobile communication scheme [6]. Modulation of amplitude in OFDM delivered huge spectrum effectiveness, less side lobe, and interference of narrowband [7]. To acquire effective transmission power, High Power Amplifier (HPA) is majorly used in wireless communication. To fulfill high yield response, HPA is majorly processed near saturated areas [8-10]. If the PAPR value is maximized in OFDM, a distortion

is obtained in channels and a high OFDM PAPR signal is obtained in multiple carrier modulation methods while summing several independent symbols [11].

While changing the process limit of the amplifier from linear to non-linear area, PAPR is created. In the transmitter end, whether the OFDM signal traveled through nonlinear HPA, the OFDM signal is clipped due to high PAPR. High PAPR reduced the process of HPA to amplify [12]. Generally, metaheuristic techniques are utilized to reduce implementation time and costs, because of their accurate engineering [13]. Hence, it faces issues like initial convergence, less search constancy, the trap of local optimal, inefficient search, and less population diversity and diverging from a solution of optimum [14]. Some of the above-mentioned issues are also presented in a traditional SCSSO algorithm [15, 16]. To overcome the limitations, the SCSSO is a hybrid with chaotic maps. The chaotic maps have benefits like local area

escaping and fastening process of search with its dynamic behavior. The SCSO has a balanced and rational rate of convergence, that performed well in identifying global optimal which affected the convergence rate. Additionally, the predators are blind because of random operating mechanisms and hence there is an incomplete exploitation rate in search space. Hence, the concept of chaos is implemented in this research named CSCSO for reducing this deficiency and maximizing efficiency. The PTS algorithm is used as PAPR reduction method in this research and for optimizing the phase factors in PTS algorithm proposed an PTS - CSCSO algorithm which reduces the PAPR in CF-OFDM. The PTS in OFDM signals and default PTS faced huge complexity in computation because of phase factor probable combinations. Low search difficulty in various optimization algorithms is currently used for optimizing PTS technique for the PAPR reduction in OFDM.

The main contribution of this research is

- Sand Cat Swarm Optimization (SCSO) algorithm with Chaotic maps is proposed to reduce PAPR values in the CP-OFDM system.
- In the Partial Transmit Sequence, the phase factor is optimized by the proposed PTS - CSCSO algorithm to reduce the PAPR values in the CP-OFDM system.
- The Space Time Block Coding (STBC) and Quadrature Amplitude Modulation (QAM-16) are utilized for encoding and decoding, modulation and demodulation process respectively.

The remaining section of the manuscript is organized in the following format: Section 2 describes literature review of PAPR reduction. Section 3 describes the details of the proposed methodology. Section 4 describes the results and discussion and section 5 concludes a manuscript.

2. Literature review

In this section, the researchers that involved in applying optimization algorithms for improving OFDM performance. The recent researches in the optimization of OFDM were analyzed in this section.

Abdul Azeez [17] implemented a Prime Learning Ant Lion Optimization (PL-ALO) technique for reducing PAPR and BER. In the implemented method, the selection method was utilized to maximize exploitation linked to a superior fitness agent which enhances the implemented method's performance. The selection method randomly performed tournaments between superior fitness search agents in method. Square-root raised Cosine

(SRC) precoding and Mu law methods were utilized to enhance a system's efficiency. The implemented method balanced a exploration and exploitation of phase factors. However, the method has less exploitation capacity and premature convergence in optimization.

Sivakumar [18] introduced the Phase Optimizer-assisted Partial Transmit Sequence (PO-PTS) method to minimize PAPR in the OFDM system. The introduced method after validation, depended on simulation outputs which were developed by Xilinx method generation in Field Programmable Gate Array (FPGA). PO was assigned for selecting optimum phase weighting factors for performing scaling through data sequence in the PTS method. The introduced method minimized execution complexity and redundancy in candidate signals. The introduced method needed an exceptional cost of PAPR and low iterations. However, the method simply falls to the local optimum in huge dimensional data and less convergence.

Abdelfatah Mohamed [19] presented a Long Short-Term Memory-Autoencoder (LSTM-AE) method for PAPR reduction in visible light communication. The presented method was used as an autoencoder and LSTM learned a complex representation of input, allowed the method to manage variable length input sequences, and also produced variable length output sequences. The presented method has an exhaustive search of the PTS phase and minimized method complexity. However, the method has less exploitation because of position discretizing.

Ch. Thejesh Kumar [20] suggested an Ant Colony Optimization (ACO) method for reducing PAPR values. The Partial Transmit Sequence (PTS) method to diminish a PAPR of the FBMC-OQAM method was implemented. The PTS method was integrated with an optimization method that supports minimizing PAPR to a higher extent to reduce the PAPR values of each block and optimize each unit. The suggested method minimizes extended peaks within FBMC-OQAM methods. The suggested method efficiently identified the space of all sequences of a given phase factor. However, the method has less convergence, exploitation rate and stagnation stage.

Shicheng Hu [21] developed a Selected Mapping (SLM) method to reduce the PAPR values. The developed method required no explicit side data transmission in OFDMA systems. The data transmitted to various UEs were employed in a set of Resource Units (RUs). The pilots were available in every RU to estimate the channel. The developed method has a huge convergence rate and execution

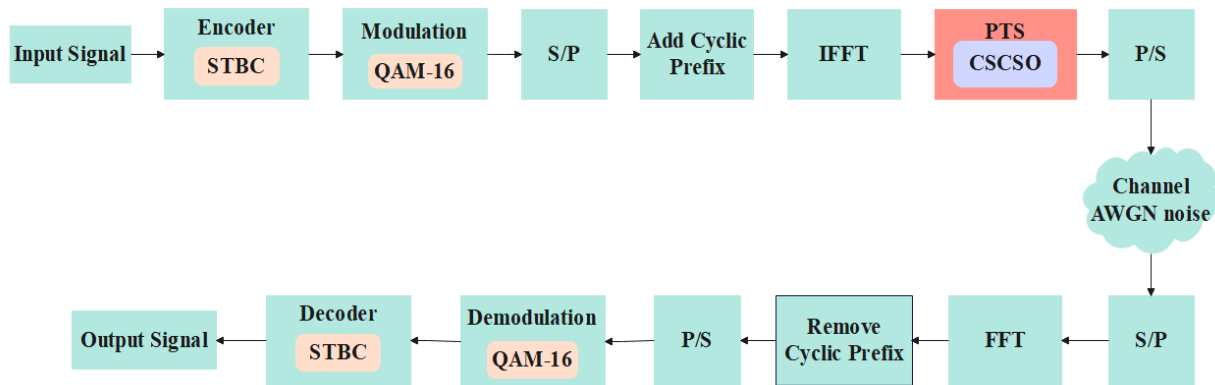


Figure. 1 Represents the process of the proposed technique

complexity depends on the estimation of the phase factor. However, the technique suffered from unbalanced exploitation, exploration and less convergence.

Prabal Gupta [22] implemented a Partial Transmit Sequence-Centering Phase Sequences Matrix (PTS-CPSM- Algo) Algorithm. The implemented method chose the superior sequences phase which reduced the PAPR which was acquired. The implemented method was very flexible for implementation and possessed huge potential. The implemented method efficiently identified the space of all sequences of a given phase factor. However, the method easily falls to the local optimum in huge dimensional data and less convergence. The existing methods have limitations of less exploitation capacity and premature convergence in optimization, easily falling to local optimum in huge dimensional data and convergence, has less exploitation because of position discretizing and easily falls to local optimum in huge dimensional data. To overcome the above limitations of existing methods, the CSCSO is a hybrid with chaotic maps. The chaotic maps have benefits like local area escaping and fastening process of search with its dynamic behavior.

3. Proposed methodology

In this research, the Partial Transmit Sequence Chaotic Sand Cat Swarm Optimization (PTS-CSCSO) technique to reduce the PAPR in the CP-OFDM system. To encode input signals Space Time Block Coding (STBC) technique and for modulation the Quadrature Amplitude Modulation (QAM-16) technique. In PTS, the phase factor is optimized by the proposed CSCSO algorithm. Fig. 1 represents the process of the proposed technique.

The process of the CP-OFDM system in the communication is described below as step by step:

- Initially, the input signals are encoded by the STBC technique which compensates for the added noise and other losses by spatial channels and minimizes bit error rates modulated by using the QAM-16 technique which efficiently modulates the signals due to their huge data rates and noise immunity.
- Next, modulated signals are given to the Serial to Parallel (S/P) process and the Cyclic Prefix (CP) which is guard interval to avoid overlapping and Inverse Fast Fourier Transform (IFFT) is performed which converts the frequency domain to the time domain.
- Next PTS phase, in that the phase factors are optimized and the best phase factor by the proposed PTS-CSCSO algorithm, again Parallel to the Serial (P/S) process is applied.
- Next, these signals are transmitted through the AWGN channel which is a basic noise method utilized in wireless communication to transmit signals, and then the S/P process is again applied, next FFT is performed that converts the time to the frequency domain.
- Then, some cyclic prefixes are removed and then demodulation and decoding processes are performed to acquire an output signal.

3.1 System model

The system model of CP-OFDM is described here, which is a particular form of OFDM used in 5G NR downlink. CP-OFDM is a superior choice for 5G-enhanced Mobile Broad Band (eMBB). To transmit downlink, the waveform of CP-OFDM is used through Long-Term EVolution (LTE). The community of mobile communication has abundant waveform proposals for roads in NR to 5G. Due to differences in CP-OFDM, many proposals are modified with multiple carrier waveforms. The final phase of CP-OFDM of information of OFDM edge is

added at the beginning of the OFDM frame and the length of CP must be higher than the delay of channel spread for solving inter-symbol interference (ISI) and inter-band interference. The subcarriers of orthogonal are developed through IFFT utilized in CP-OFDM. Symbols of data have references that are transmitted to the time domain and transferred through addition of CP. Initially, modified Symbol (STO) and Carrier Frequency Offset (CFO) modifications from channel to receiver. The transferred signal is returned utilizing FFT, at last, equalization-based reference symbols are utilized to perform channel evaluation.

Consider, L as the number of subcarriers and L_{CP} represents the length of CP. To ignore ISI in OFDM, CP is combined with every OFDM symbol. $L_b = L_{cp} + L$ represents the block length of every OFDM symbol. The mathematical formula for CP-OFDM symbol discrete-time received in CFO and ACI is given as Eq. (1),

$$Y = \Omega_r h \Gamma(\varepsilon) \Omega_t V^H S + M + A(\psi, K) \quad (1)$$

Where, Ω_r represents the elimination matrix of CP, h represents the channel vector, $\Gamma(\varepsilon)$ represents a matrix of CFO, Ω_t represents the matrix of CP insertion, V represents the matrix of Fourier, S represents the sequence of transmitted symbol, M represents Independent Identically Distributed (IID) and $A(\psi, K)$ represents components of ACI and ψ represents sentry band in mid-CP-OFDM. The mathematical formula of S , Ω_t and $\Gamma(\varepsilon)$ is given as Eqs. (2), (3), and (4) respectively.

Where,

$$S = [S(0), S(1), \dots, S(L-1)]^T \quad (2)$$

$$\Omega_t = \begin{bmatrix} 0 & I_{L_{cp}} \end{bmatrix} I_L \quad (3)$$

$$\Gamma(\varepsilon) = \text{diag} \left[1, e^{\frac{2\pi\varepsilon}{L}}, \dots, \infty, e^{\frac{2\pi(L-1)\varepsilon}{L}} \right] \quad (4)$$

Where, $\varepsilon = \frac{f_n}{\Delta f_n} = \frac{f_n}{f_n - f_{nr}}$ represents normalized frequency, f_{nt} and f_{nr} represents carrier frequency at receiver. The initial column d represented as $[d(0), d(1), \dots, d(F-1), 0, \dots, 0]$ represents channel gain $d(l)$ in matrix of Toeplitz channel. The mathematical formula of $Z(\Psi, K)$ is given as Eq. (5),

$$Z(\Psi, K) = \sum_{i=1}^i \alpha_{cp}(\Psi, i) \Omega_r d^{ik} \Gamma(\varepsilon^{ik}) \Omega_t V^H S_i \quad (5)$$

Where, d^i represents in among channel target receiver and ith user, respective ith transmitted

signal of user and matrix of CFO is described as S_i and $\Gamma(\varepsilon^{ik})$. In the frequency domain, the mathematical formula for the acquired signal is given as Eq. (6),

$$r = DOS + M + A \quad (6)$$

The system model for PAPR is described in the below section.

3.1.1 PAPR

The continuous time of OFDM signal is given as Eq. (7),

$$s(t) = \frac{1}{L} \sum_{k=0}^{L-1} S_{m,k} \exp(j2\pi f_{nk} t) \quad (7)$$

Where,

$S_m = [S_{m,0}, S_{m,1}, \dots, S_{m,L-1}]$ represents the m th OFDM symbol vector. The Quadrature Amplitude Modulation (QAM-16) is used for modulating every element of the relative vector. Frequency of $f_{ni} = i\Delta f_n$, $0 \leq i \leq L-1$ that is employed to symbol vector of OFDM in ith unit. Δf represents subcarrier spacing. The mathematical formula for the oversampling process in discrete-time OFDM signal is given as Eq. (8),

$$s_m(l) = \frac{1}{\sqrt{L}} \sum_{k=0}^{L-1} S_{m,i} \exp\left(\frac{j2\pi l i}{FL}\right) \quad 0 \leq l \leq FL-1 \quad (8)$$

Where, F represents the factor of oversampling. The process of oversampling in CP-OFDM system is symbol vectors of oversampled OFDM is continued from FL length to span of $2M + CP + FL$ through enforcing the extension of overlap and CP operations. After the process of CP and overlap extension, m th CP-OFDM symbol is given as Eq. (9),

$$r_m[l] = \begin{bmatrix} x_m[FL - CP - M], s_m[FL - CP - M + 1], \dots, [s_m[FL - 1]], s_m[0], s_m[1], \dots, s_m[FL - 1], s_m[0], s_m[1], \dots, s_m[M - 1]] \end{bmatrix} \quad 0 \leq l \leq 2M + CP + FL - 1 \quad (9)$$

To estimate the signal's dynamic range $v(l)$, a PAPR of CP-OFDM is utilized and a mathematical formula is given as Eq. (10),

$$PAPR [v[l]] = \frac{\max_{0 \leq l \leq M(CP+FL+M)+M-1} |s[l]|^2}{E[|v[l]|^2]} \quad (10)$$

Where $E[\cdot]$ represents expectation operation. The performance of PAPR reduction is calculated through the Complementary Cumulative Distribution Function (CCDF) of PAPR. CCDF represents the probability which PAPR of the OFDM symbol exceeds a prearranged threshold $PAPR_0$ and mathematical formula for CCDF (PAPR) is given as Eq. (11),

$$CCDF(PAPR_0) = \Pr (PAPR > PAPR_0) \quad (11)$$

Generally, for OFDM systems with samples of Gaussian time domain, the mathematical formula of CCDF of PAPR is given as Eq. (12),

$$Pr = (PAPR > PAPR_0) = 1 - (1 - e^{-PAPR_0})^l \quad (12)$$

The process of encoding, decoding and modulation, demodulation process are described in the below sections.

3.2 Encoding and decoding

The technique used for encoding and decoding a signal is Space Time Block Coding (STBC) which transmits that data to enhance data transfer reliability. Consider a quasi-static flat fading channel with N_t which is a transmitter and N_r which is the receiver,

next received signal vector $Y^t = \begin{bmatrix} Y_1^t \\ \dots \\ Y_{N_r}^t \end{bmatrix}$ at time t is given as Eq. (13),

$$Y^t = HX^t + Noise \quad (13)$$

Where, $X^t = \begin{bmatrix} x_1^t \\ \dots \\ x_{N_t}^t \end{bmatrix}$ represents the transmitted

signal vector at time t and H represents $N_r \times N_t$ difficult number channel coefficient matrix. To assumption of quasi-static, channel reaction is modifying at random among adjacent blocks, hence it is not variable in transmission time and that time is called coherence time. The mathematical formula for encoding matrix in STBC is given in Eq. (14),

$$G = \begin{pmatrix} S_1 & S_2 & S_3 & S_4 \\ -S_2 & S_1 & -S_4 & S_3 \\ -S_3 & S_4 & S_1 & -S_2 \\ -S_4 & -S_3 & S_2 & S_1 \\ S_1^* & S_2^* & S_3^* & S_4^* \\ -S_2^* & S_1^* & -S_4^* & S_3^* \\ -S_3^* & S_4^* & S_1^* & -S_2^* \\ -S_4^* & -S_3^* & S_2^* & S_1^* \end{pmatrix} \quad (14)$$

Where, S_1, S_2, S_3 and S_4 represents the modulated signal of STBC encoder and the sequence of two signals of transmitters is orthogonal. Next, for the decoding process in STBC technique, channel coefficients should be evaluated next Maximum Ratio Combiner (MRC) decoder evaluates actual signals S_1, S_2, S_3 and S_4 through integrating received signal vectors Y^t at time t utilizing linear transformation and a mathematical formula is given in Eq. (15),

$$\begin{bmatrix} Y^1 \\ Y^2 \\ Y^3 \\ Y^4 \\ (Y^5)^* \\ (Y^6)^* \\ (Y^7)^* \\ (Y^8)^* \end{bmatrix} = \begin{pmatrix} h_1 & h_2 & h_3 & h_4 \\ h_2 & -h_1 & h_4 & -h_3 \\ h_3 & -h_4 & -h_1 & h_2 \\ h_4 & h_3 & -h_2 & -h_1 \\ h_1^* & h_2^* & h_3^* & h_4^* \\ h_2^* & -h_1^* & h_4^* & -h_3^* \\ h_3^* & -h_4^* & -h_1^* & h_2^* \\ h_4^* & h_3^* & -h_2^* & -h_1^* \end{pmatrix} \begin{bmatrix} S_1 \\ S_2 \\ S_3 \\ S_4 \end{bmatrix} + noise \quad (15)$$

Where, h_i represents i th column of channel coefficient matrix H . Generally, the mathematical equation of MRC for orthogonal STBC is given in Eq. (16),

$$Y_{MRC} = H_{MRC} \times \begin{bmatrix} S_1 \\ \dots \\ S_4 \end{bmatrix} + noise \quad (16)$$

From above Eq. (16), the HMRC is an orthogonal matrix that made input data symbols of STBC, and the mathematical formula of the decoding process is given in Eq. (17),

$$\begin{bmatrix} \check{S}_1 \\ \dots \\ \check{S}_2 \end{bmatrix} \cong \frac{1}{\|H_{MRC}\|} (H_{MRC})^H Y_{MRC} \quad (17)$$

From the above Eq. (17), it is clear that the performance of STBC counts effectively on the quality of the channel estimator. The encoded signals are transmitted to the QAM- 16 modulation method to modulate the signal.

3.3 Modulation and demodulation

The technique used for modulation and demodulation is Quadrature Amplitude Modulation (QAM-16) which utilizes two independent digital baseband signals for modulation of equally orthogonal two-band and similar frequency carrier signals. Modulated signals have similar bandwidth in orthogonal. To attain two-stage parallel digital signal transmission in quadrature and phase. The

mathematical formula for the QAM-16 signal is given in Eq. (18),

$$S_{QAM}(t) = \sum_n A_n g(t - nT_S) \cos(\omega_c t + \theta_n) \quad (18)$$

Where, A_n represents the amplitude of the baseband signal, $g(t - nT_S)$ represents the single waveform of the baseband signal, T_S represents width. The mathematical representation of the above formula in orthogonal representation is given in Eq. (19),

$$S_{QAM}(t) = [\sum_n A_n g(t - nT_S) \cos \theta_n] \cos \omega_c t - [\sum_n A_n g(t - nT_S) \sin \theta_n] \sin \omega_c t \quad (19)$$

Then, the mathematical formula of above Eq. (19) is modified in Eq. (20),

$$S_{QAM}(t) = X(t) \cos \omega_c t - Y(t) \sin \omega_c t \quad (20)$$

The amplitude in QAM-16 Y_n is represented as Eq. (21),

$$\begin{cases} X_n = c_n A \\ Y_n = d_n A \end{cases} \quad (21)$$

Where, A, c_n and d_n represents fixed amplitude which is determined through the input signal. The coordinate point of QAM-16 signal in space of signal is adjusted through c_n and d_n . The modulated signal is converted to parallel from serial, then add cyclic prefix which is guardian interval to avoid overlap, and next the signal is transmitted to the PTS method.

3.4 Partial transmit sequence

The PTS technique separates input data blocks to disjoint sub-blocks, executes IFFT of subblocks, rotates sub-blocks with relevant phase factors, and merges them to form transmitted signals. PTS technique is utilized majorly for the mitigation of peak power problems in signals of OFDM. That is processed at cost of maximized exceptional difficulty as count of sub-blocks maximizes. In this research, input data block X is divided into L sub-blocks, and the vector depiction is given in Eq. (22),

$$X^l = \{X_0^l X_1^l X_2^l \dots X_{K-1}^l\} \quad (22)$$

The mathematical formula for adding all sub-blocks is represented in Eq. (23),

$$X = \sum_{l=0}^{L-1} X^l \quad (23)$$

Here, X is the output sub-blocks X^l in the domain of frequency that is next returned to the time domain through IFFT. It results next process phase rotation through a count of factors given in Eq. (24),

$$B_l = \exp(j\phi_l), \phi_l \in \left\{ \frac{2\pi n}{W_{ph}} \mid n=0,1,\dots,W_{ph}-1 \right\} \quad (24)$$

The aim is to minimize *PAPR* of entire L sub-blocks through phase rotation and integrate it through P/S conversion that gives OFDM signal to \tilde{x} is given in Eq. (25),

$$\tilde{x} = \sum_{l=0}^{L-1} B_l x^l \quad (25)$$

Considering that W_{ph} phase angles are only permitted, next its kinds $P = W_{ph}^L$ single OFDM symbols as their result.

In PTS, a consecutive procedure of phase factor search for less *PAPR* is difficult because of the huge count of sub-carriers. In phase factor search procedure, proposed technique combines vectors of phase factor attaining less *PAPR* which is considered an NP-complete combinatorial optimization (CO) issue. The comprehensive search of phase factors in the optimum, PTS method is not suitable because of high computational complexity. Hence, a CSCSO algorithm is introduced to overcome the limitation.

3.4.1 Chaotic sand cat swarm optimization algorithm

Existing optimization algorithms faced issues like initial convergence, less search constancy, the trap of local optimal, incompetent search and less population diversity. Some of mentioned issues exist in traditional SCSO algorithms. To overcome these above-mentioned limitations, the SCSO is a hybrid with chaotic maps. To obtain lower *PAPR* values in difficult sub-carrier systems, a better optimization algorithm is required. In this research, Chaotic Sand Cat Swarm Optimization (CSCSO) technique as an optimization method to acquire less *PAPR* values. The major process of a CSCSO algorithm is to combine chaos features of non-reducing positions to the core search process of SCSO for improving a performance of global search. The proposed algorithm is dependent on probability distribution and random behavior is the main advantage when using chaotic concepts. So, the proposed algorithm enhanced a convergence rate through utilizing chaotic maps and escaped from local traps much easily than traditional algorithms. The randomness in a SCSO algorithm is replaced through a chaotic map because of the same randomness features with superior and dynamic properties. In the CSCSO

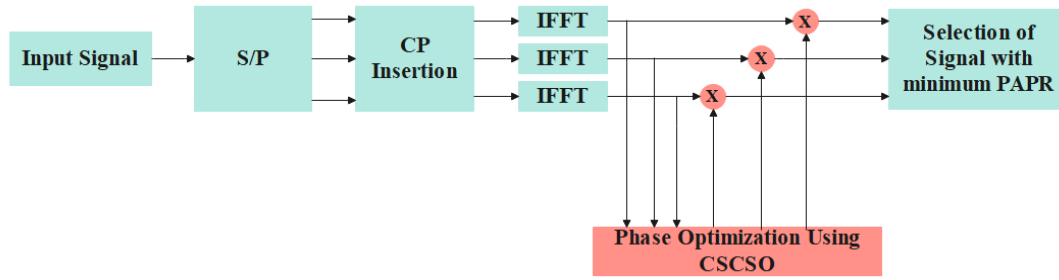


Figure. 2 Represents the workflow of proposed CSCSO algorithm

algorithm, there are 12 chaotic maps are given for tuning a step size of traditional SCSO algorithm that maximizes population spread probability and attains much more robust and balanced solutions. Fig. 2 represents the workflow of the proposed CSCSO algorithm.

In this research, a proposed algorithm introduced two various solutions for location updates in phases. One is a normal mechanism's location update and the next is dependent on the chaotic method. The mathematical formula has a 50% chance of balancing weight and is given as Eq. (26),

$$\vec{X}(t + 1) = \begin{cases} \text{if } p < 0.5 \\ \text{if } p \geq 0.5 \end{cases} \quad 1 \quad (26)$$

Where p represents the random value among 0 and 1. The main essential parameter to perform the same task in the SCSO algorithm is C parameter. The parameter played an essential part in exhibiting a fair and balanced behavior for exploitation and exploration but might face less convergence and unsuccessful exploitation, particularly in difficult and constrained issues. Following Eqs (27) and (28) are used to enhance the process of exploration and exploitation stages

$$s = 2^k; \quad k \geq 1 \quad (27)$$

$$C = s - s \frac{\sqrt[7]{e^t - 1}}{e - 1} \quad (28)$$

Where K represents the constant coefficient. The parameter K played an essential part in the algorithm weight given to every phase. The C parameter is essential to make the CSCSO algorithm much easier because that played one role in the exploitation and exploration stages. Parameters R and r are affected by new equation. Parameter R depended on C , their fluctuation range is minimized. R represents random value in a interval $[-2C, 2C]$. CSCSO technique forced search agent while R is less than or similar to

1 or else search agent is required for explore and identify prey. The R and r parameters for obtaining through effect of chaotic maps are measured by eqns (29) and (30),

$$\vec{R} = 2 \times \vec{c} \times m - \vec{c} \quad (29)$$

$$\vec{r} = \vec{c} \times m \quad (30)$$

$$\vec{X}(t + 1) = \begin{cases} \vec{X}_b(t) - \vec{X}_{rnd} \cdot \cos(\theta) \cdot \vec{r} & |R| \leq 1(a) \\ \vec{r} \cdot (\vec{X}_c(t) - m \cdot \vec{X}_t(t)) & |R| > 1(b) \end{cases} \quad (31)$$

Where, m represents chaotic vector which is measured depending on the chaotic map. Mathematical formula for CSCSO is measured following Eq. (31) as given before. In different issues, particularly constrained optimization issues, that can identify other probable local areas in global space by quick and precise convergence because of a proposed CSCSO algorithm's behavior. Proposed method enhances SCSO's performance when similar to the actual SCSO algorithm concerning difficulty analysis. At last, optimum phase factors are acquired through optimization, additionally, that provides high optimum phase factors due to PTS-CSCSO.

4. Experimental results

The proposed PTS-CSCSO algorithm is simulated on MATLAB R2021b version 9.11 with

Table 1. Parameter setting

Parameter	Value
No. of iterations	100
Population size	30
FFT size	64, 128, 256, 512, 1024
No. of subcarriers	64, 128, 256, 512, 1024
Cyclic Prefix	0 to 2e-6s
Modulation	16 QAM
Modulation range	16
Channel type	AWGN channel

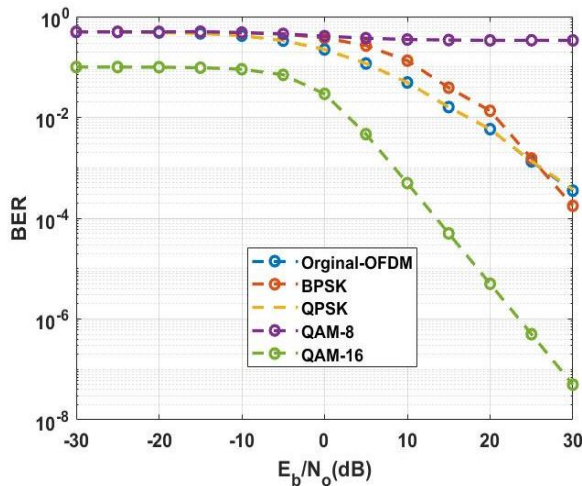


Figure. 3 Performance of QAM-16 with BER

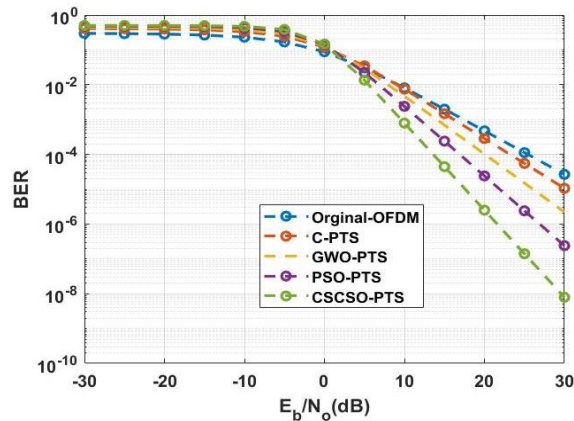


Figure. 4 Performance of CSCSO with BER

system requirements of i5 processor and 6GB RAM. The performance of a proposed algorithm is evaluated with performance measures BER, SER and CCDF. The performance of utilized QAM-16 modulation is evaluated with existing methods like default OFDM, Binary Phase Shifting Keying (BPSK), Quadrature Phase Shifting Keying (QPSK) and 8-order QAM. The performance of proposed CSCSO algorithm is analyzed with existing methods like default OFDM, Conventional- (C-PTS), Grey Wolf Optimization (GWO-PTS) and Particle Swarm Optimization (PSO-PTS). The parameter setting of the method is described in Table 1.

4.1 Quantitative and qualitative analysis

The performance of a proposed algorithm is analyzed with performance measures of BER, CCDF and SER. The utilized QAM-16 and proposed PTS-CSCSO algorithm are evaluated with various existing techniques for different PAPR (dB). Different pictorial representations are described in this section

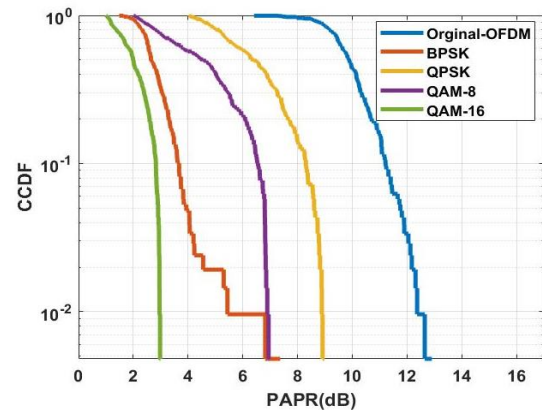


Figure. 5 Performance of QAM-16 with PAPR

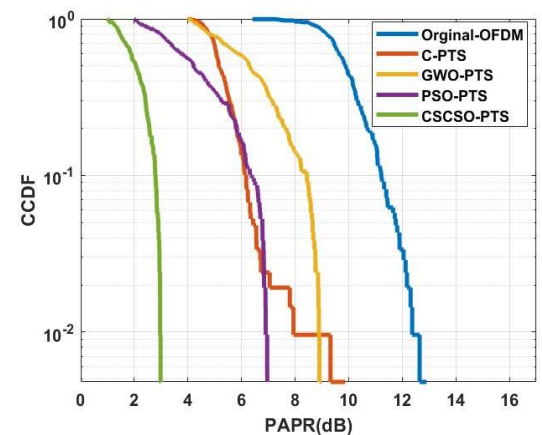


Figure. 6 Performance of CSCSO with PAPR

to show the superior performance of the proposed algorithm.

Figs. 3 and 4 represent the performance of QAM-16 and PTS-CSCSO algorithm with respect to BER respectively. From Fig. 3, it is clear that the QAM-16 attained less BER which is superior to other existing modulation techniques like default OFDM, BPSK, QPSK and QAM-8. From Fig. 4, it is clear that the proposed PTS-CSCSO algorithm attained less BER which is superior to other existing PAPR reduction techniques.

Figs. 5 and 6 represent the performance of QAM-16 and PTS-CSCSO algorithm with respect to CCDF respectively. From Fig. 5, it is clear that the QAM-16 attained less CCDF which is superior to other existing modulation techniques like default OFDM, BPSK, QPSK and QAM-8. From Fig. 6, it is clear that the proposed PTS-CSCSO algorithm attained less CCDF which is superior to other existing PAPR reduction techniques.

Figs. 7 and 8 represent the performance of QAM-16 and PTS-CSCSO algorithm concerning SER respectively. From Fig. 7, it is clear that the QAM-16 attained less SER which is superior to other existing

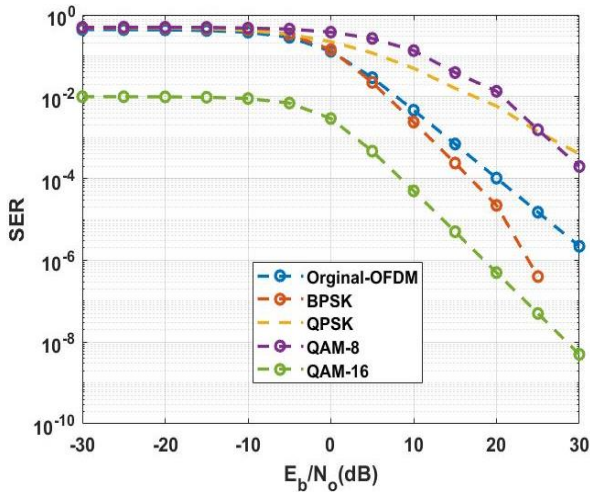


Figure. 7 Performance of QAM-16 with SER

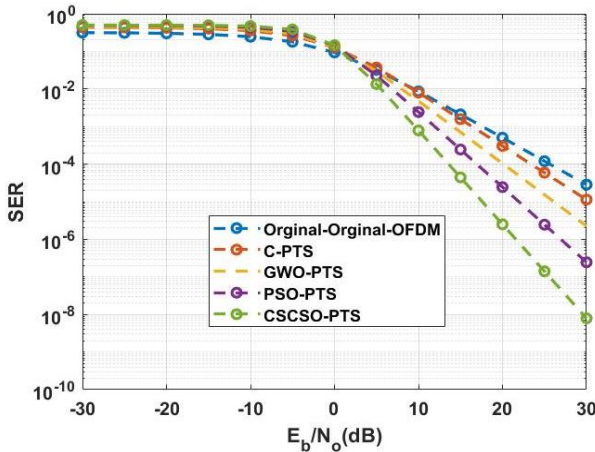


Figure. 8 Performance of CSCSO with SER

modulation techniques like default OFDM, BPSK, QPSK, and QAM-8. From Fig. 8, it is clear that the proposed PTS-CSCSO algorithm attained less SER which is superior to other existing PAPR reduction techniques.

4.2 Comparative analysis

The performance of a developed PTS - CSCSO algorithm is compared to other previous techniques such as PO-PTS [18], LSTM-AE [19], ACO [20], SLM [21] and PTS-CPSM-Algo [22].

In Table 2, performance of proposed algorithm is compared to PO-PTS [18] method for 512 subcarriers,

Table 2. Comparative analysis of proposed method at 16 QAM

Author	Method	SNR (E_b/N_0) in dB
Sivakumar [18]	PO-PTS	21.48
Proposed algorithm	PTS - CSCSO	20.32

Table 3 Comparative analysis of proposed method at $CCDF = 10^{-3}$

Author	Method	PAPR (dB)
Abdelfatah Mohamed [19]	LSTM-AE	10.3
Proposed algorithm	PTS - CSCSO	3.01

Table 4 Comparative analysis of proposed method with SNR

Author	Method	BER	
		SNR = 10 dB	SNR = 30 dB
Abdelfatah Mohamed [19]	LSTM-AE	7×10^{-1}	3×10^{-3}
Proposed Algorithm	PTS - CSCSO	7×10^{-4}	2×10^{-4}

Table 5 Comparative analysis of proposed method with SNR

Author	Method	BER	
		SNR = 10 dB	SNR = 30 dB
Ch. Thejesh Kumar [20]	PTS - ACO	4×10^{-3}	N/A
Proposed Algorithm	PTS - CSCSO	7×10^{-4}	2×10^{-4}

16-QAM and Rayleigh Fading channel. For 16-QAM, the proposed method attained 20.32 dB while PO-PTS [18] attained 21.48 dB.

In Table 3, performance of proposed method is compared with LSTM-AE [19] method for 16-QAM, 256 subcarriers and AWGN channel. At $CCDF = 10^{-3}$, the proposed method attained 3.01 PAPR while LSTM-AE [19] attained 10.3 PAPR.

In Table 4, performance of proposed method is compared with LSTM-AE [19] method for 16-QAM, 256 subcarriers and AWGN channel. At SNR= 10 dB, proposed algorithm reached BER of 7×10^{-4} and at SNR = 30 dB, proposed algorithm reached BER of 2×10^{-4} while [19] reached 7×10^{-1} and 3×10^{-3} BER.

Table 6 Comparative analysis of proposed method with SNR

Author	Method	BER	
		SNR = 10 dB	SNR = 30 dB
Shicheng Hu [21]	SLM	4×10^{-1}	5×10^{-3}
Proposed Algorithm	PTS - CSCSO	7×10^{-4}	2×10^{-4}

Table 7 Comparative analysis of proposed method with subcarriers

Author	Method	PAPR (dB)	
		128	256
Prabal Gupta [22]	PTS-CPSM- Algo	6.93	7.54
Proposed Algorithm	PTS - CSCSO	3.01	4.12

In Table 5, performance of proposed method is compared with PTS - ACO [20] method for 64 subcarriers and AWGN channel. At SNR= 10 dB, proposed algorithm reached BER of 7×10^{-4} and at SNR = 30 dB, proposed algorithm reached BER of 2×10^{-4} while [20] reached 4×10^{-3} BER.

In Table 6, performance of proposed method is compared with PTS - CPSM -Algo [21] method for 16-QAM and 1024 subcarriers. At SNR= 10 dB, proposed algorithm reached BER of 7×10^{-4} and at SNR = 30 dB, proposed algorithm reached BER of 2×10^{-4} while [21] reached 4×10^{-1} and 5×10^{-3} BER.

In Table 7, performance of proposed algorithm is compared to PTS-CPSM-Algo [22] method. At 128 subcarriers, the proposed method attained 3.01 PAPR while PTS-CPSM-Algo [22] method attained 6.93 PAPR. At 256 subcarriers, the proposed method attained 4.12 PAPR while PTS-CPSM-Algo [22] method attained 7.54 PAPR.

In this section, the limitations of existing methods and advantages of the proposed PTS-CSCSO algorithm to reduce PAPR reduction in the CP-OFDM system. The PO-PTS [18] method has the drawback of less exploitation capacity and premature convergence in optimization. The LSTM-AE [19] method has the drawback of easy falls to local optimum in huge dimensional data and less convergence. The ACO [20] method has less exploitation because of position discretizing. The SLM [21] technique has the drawback of less convergence, exploitation rate, and stagnation stage. The PTS-CPSM-Algo [22] technique has the drawback of suffering from unbalanced exploitation, exploration and less convergence. To overcome these limitations, the CSCSO is a hybrid with chaotic maps. The chaotic maps have benefits like local area escaping and fastening the search process with its dynamic nature.

5. Conclusion

To reduce PAPR values, this research proposed a PTS-CSCSO algorithm of CP-OFDM. To encode and decode the signal in the CP-OFDM system, the STBC technique is utilized. For modulation and demodulation, the QAM-16 method is utilized. The

PTS technique is utilized for PAPR reduction, in that the phase factor is optimized by using the proposed PTS-CSCSO algorithm. The AWGN channel with noise is utilized, that transmit the signal from transmitter to receiver. On the receiver end, S/P conversion, FFT are utilized to receive signals and that are demodulated and decoded to obtain output signals. The performance of a proposed algorithm is analysed with performance metrics of BER, SER, and CCDF. The proposed method attained less PAPR of 3.01 dB at 128 subcarriers and 4.12 dB at 256 subcarriers. When SNR =10 dB, proposed algorithm reached less BER of 7×10^{-4} and SNR = 30 dB proposed algorithm reached BER of 2×10^{-4} which is more effective than other existing methods. In the future, hybrid or integration of different PAPR reduction techniques can be used for PAPR reduction in the CP-OFDM system.

Notation

Notations	Description
L	Number of subcarriers
L_{CP}	Length of CP
Ω_r	Elimination matrix of CP
h	Channel vector
$\Gamma(\varepsilon)$	Matrix of CFO
Ω_t	Matrix of CP insertion
V	Matrix of Fourier
S	Sequence of transmitted symbol
M	Independent Identically Distributed
$A(\psi, K)$	Components of ACI
ψ	Sentry band in mid-CP-OFDM
$\varepsilon = \frac{f_n}{\Delta f_n} = \frac{f_n}{f_n - f_{nr}}$	Normalized frequency
f_{nt} and f_{nr}	Carrier frequency at receiver
d^i	Channel target receiver and i th user
S_i	User signal
$\Gamma(\varepsilon^{ik})$	Matrix of CFO
S_m	m th OFDM symbol vector
Δf	Subcarrier spacing
F	Factor of oversampling
$v(l)$	Signal's dynamic range
$E[\cdot]$	Expectation operation
N_t	Transmitter
N_r	Receiver
X^t	Transmitted signal vector
H	Difficult number channel coefficient matrix
S_1, S_2, S_3 and S_4	Modulated signal of STBC encoder
h_i	i th column of channel coefficient matrix H
A_n	Amplitude of the baseband signal

$g(t - nT_s)$	Single waveform of the baseband signal
T_s	Width
A, c_n and d_n	Fixed amplitude
X	Input data block
W_{ph}	Phase angles
p	Random value among 0 and 1
K	Constant coefficient
m	Chaotic vector

Conflicts of Interest

The authors declare no conflict of interest.

Author Contributions

The paper conceptualization, methodology, software, validation, formal analysis, investigation, resources, data curation, writing—original draft preparation, writing—review and editing, visualization, have been done by 1st author. The supervision and project administration, have been done by 2nd author.

References

- [1] C. Sun, J. Zhao, J. Wang, L. Xia, X. Gao, and Q. Wang, “Beam Domain MIMO-OFDM Optical Wireless Communications with PAPR Reduction”, *IEEE Photonics Journal*, Vol. 15, No. 2, pp. 1-10, 2023.
- [2] G. Harish Kumar, and P.T. Rao, “An energy efficiency perceptible on MIMO-OFDM systems using hybrid fruit fly-based salp swarm optimization technique”, *Concurrency and Computation: Practice and Experience*, Vol. 35, No. 1, pp. e7416, 2023.
- [3] Z. Liu and M. Ma, “Deep Learning-Based Joint Optimization of Modulation and Power for Nonlinearity-Constrained System”, *IEEE Access*, Vol. 10, pp. 30018-30025, 2022.
- [4] S. Carcangiu, A. Fanni, and A. Montisci, “A Closed Form Selected Mapping Algorithm for PAPR Reduction in OFDM Multicarrier Transmission”, *Energies*, Vol. 15, No. 5, pp. 1938, 2022.
- [5] N. A. Sivadas, “PAPR reduction of OFDM systems using H-SLM method with a multiplierless IFFT/FFT technique”, *ETRI Journal*, Vol. 44, No. 3, pp. 379-388, 2022.
- [6] L. Li, L. Xue, X. Chen, and D. Yuan, “Partial transmit sequence based on discrete particle swarm optimization with threshold about PAPR reduction in FBMC/OQAM system”, *IET Communications*, Vol. 16, No. 2, pp. 142-150, 2022.
- [7] Y. Lu, F. Hu, L. Jin, J. Liu, and G. Zhang, “Continuous unconstrained PSO-PTS strategy to maximize HPA energy efficiency for FBMC-OQAM systems”, *IET Communications*, Vol. 17, No. 5, pp. 614-631, 2023.
- [8] G. Baruffa, L. Rugini, F. Frescura, and P.P. Banelli, “Low-Complexity PAPR Reduction by Coded Data Insertion on DVB-T2 Reserved Carriers”, *IEEE Access*, 2023.
- [9] Q. Nguyen, T. K. Nguyen, H. H. Nguyen, and B. Berscheid, “Novel PAPR reduction algorithms for OFDM signals”, *IEEE Access*, Vol. 10, pp. 77452-77461, 2022.
- [10] M. A. Abdelhamed, A. Zekry, S. Elagooz, and F. E. A. El-Samie, “All-Pass Filters as a Low-Complexity PAPR Reduction Scheme for SC-FDMA System”, *Wireless Personal Communications*, Vol. 124, No. 2, pp. 967-987, 2022.
- [11] J. Rong, F. Liu, and Y. Miao, “Integrated radar and communications waveform design based on multi-symbol OFDM”, *Remote Sensing*, Vol. 14, No. 19, pp. 4705, 2022.
- [12] G. Krishna Reddy and G. Merlin Sheeba, “Enhancing PAPR performance in MIMO-OFDM system using hybrid optimal MMSE-MLSE equalizers”, *Multimedia Tools and Applications*, pp. 1-21, 2023.
- [13] S. M. Farid, M. Z. Saleh, H. M. Elbadawy, and S. H. Elramly, “ASCO-OFDM based VLC system throughput improvement using PAPR precoding reduction techniques”, *Optical and Quantum Electronics*, Vol. 55, No. 5, pp. 410, 2023.
- [14] M. Liu, W. Xue, J. Gao, Y. Xu, P. Jia, and W. Chen, “Optimized baseband Nyquist pulse-based PAPR reduction method for SEFDM systems”, *Telecommunication Systems*, Vol. 81, No. 2, pp. 289-306, 2022.
- [15] M. Akurati, S. K. Pentamsetty, and S. P. Kodati, “Optimizing the Reduction of PAPR of OFDM System Using Hybrid Methods”, *Wireless Personal Communications*, Vol. 125, No. 3, pp. 2685-2703, 2022.
- [16] K. U. Chowdary and B. Prabhakara Rao, “PAPR reduction and spectrum sensing in MIMO systems with optimized model”, *Evolutionary Intelligence*, Vol. 15, No. 2, pp. 1265-1278, 2022.
- [17] A. Azeez and S. Tarannum, “Prime Learning Ant Lion Optimization with Precoding and Companding for PAPR Reduction in MIMO-OFDM”, *International Journal of Intelligent Engineering & Systems*, Vol. 15, No. 5, 2022.

- [18] S. A. Sivakumar, C. Arvind, R. Senthil Ganesh, and B. Maruthi Shankar, "FPGA Implementation of a Phase Optimizer-Assisted PTS Scheme for PAPR Reduction in OFDM Systems", *IETE Journal of Research*, pp. 1-8, 2023.
- [19] A. Mohamed, A. S. T. Eldien, M. M. Fouda, and R. S. Saad, "LSTM-Autoencoder Deep Learning Technique for PAPR Reduction in Visible Light Communication", *IEEE Access*, Vol. 10, pp. 113028-113034, 2022.
- [20] C. T. Kumar, A. Karpurapu, and Y. P. Singh, "Reduction of PAPR for FBMC-OQAM system using Ant Colony Optimisation technique", *Soft Computing*, Vol. 26, No. 9, pp. 4295-4302, 2022.
- [21] S. Hu, S. Wan, M. Yang, K. Kang, and H. Qian, "An Improved SLM Algorithm for OFDMA System with Implicit Side Information", *Journal of Signal Processing Systems*, Vol. 94, No. 8, pp. 837-846, 2022.
- [22] P. Gupta, H. P. Thethi, and A. Tomer, "An efficient and improved PTS algorithm for PAPR reduction in OFDM system", *International Journal of Electronics*, Vol. 109, No. 7, pp. 1252-1277, 2022.